Supporting Information

Highly Efficient Near-Infrared Photothermal Conversion of Single Carbon Nanocoil Indicated by Cell Ejection

Peng Wang, Lujun Pan,* Chengwei Li, Jia Zheng

School of Physic, Dalian University of Technology

No.2 Linggong Road, Ganjingzi District, Dalian, 116024, P.R. China

*Email: lpan@dlut.edu.cn   Fax: +86 0411 84709304

Table of Contents

I. Calculations and Methods

Description of Finite Element Analysis (FEA) Model. We use the Comsol Multiphysics software (Version 5.3) to build our simulation model. The FEA model is shown in Figure S1. A single CNC (the spiral line) is placed horizontally in the yeast cell solution (the cylindrical domain). The solution is treat as infinite pure water areas, the effect of cells on the properties of water is ignored because the cell concentration is very low. The mass density, thermal conductivity and specific heat capacity of CNC are considered to be 2260 kg/m³, 3 W/(m·K), and 910 J/(kg·K), respectively.[1-2] The coil diameter, line diameter, and helical pitch are 500 nm, 300 nm, 800 nm respectively. Accroding to our experimental data, the maximum velocity is lower than one millimeter per second. Thus, the Mach number (Ma) and the Reynolds number are deduced as follows,

$$Ma = v/c \approx 10^6 = 0.3 \tag{S1}$$

$$Re = \rho L v / \mu \approx 10^{-3} = 1 \tag{S2}$$

where v, c are the velocity of the solution and the sound velocity in the water, respectively. ρ, μ are the density and the dynamic viscocity, respectively, L is the typical length which is set as the line diameter of the CNC, 300 nm. Thus, in our case, the cell solution flow is treat as Stokes flow. The Navier-Stokes equation is adequate for such a microscale solid-liquid system.

Compressible Stokes flow module and liquid-solid conjugate heat transfer module are used for in this simulation. According to the heat transfer theory and fluid dynamics, the mass continuity equation in our case is written as

$$\partial \rho_s / \partial t + \nabla \cdot (\rho_s v) = 0 \tag{S3}$$

where v is the fluid speed. The compressible Navier–Stokes momentum equation is written as

$$\rho_s(\partial v / \partial t + v \cdot \nabla v) = \nabla \cdot \{-pI + \mu_s[\nabla v + (\nabla v)^T] - 2/3 \cdot \mu_s(\nabla \cdot v)I\} + \rho_s g \tag{S4}$$

where ρ_s and μ_s are the density and the dynamic viscosity of the cell solution, respectively. $\boldsymbol{I}$ is the unit diagonal matrix, p is the pressure, and $\boldsymbol{g}$ is the gravitational acceleration.

Due to the sub-microscale of the CNC (the coil diameter of CNC is lower than 1 μm), the velocity slip on the CNC-solution interface should be considered.[3-4] Thus, the boundary condition is given by second-order velocity slip boundary condition as follow[5]

$$v - v_{CNC} = \frac{2 - \sigma_v}{\sigma_v} \frac{l}{\mu} \boldsymbol{\tau}_t + \frac{3\mu}{4\rho_s T_s} [\nabla T_{CNC} - (\nabla T_{CNC} \cdot \boldsymbol{n})\boldsymbol{n}] \tag{S5}$$

where v_{CNC} is the velocity of the CNC, which is zero in our case. l is the mean free path of the water molecule, $\boldsymbol{n}$ is the boundary normal, $\boldsymbol{\tau}_t$ is the tangential viscous stress tensor. T_s and T_{CNC} are the temperature of the cell solution and the CNC, σ_v is the tangential momentum accommodation coefficient.

The heat transfer differential equation of the surrounding solution is described as

$$\rho_s C_{p,s} \partial T_s / \partial t + \rho_s C_{p,s} v \cdot \nabla T_s - \nabla \cdot (k_s \cdot \nabla T_s) = 0 \tag{S6}$$

where $C_{p,s}$ and k_s are the specific heat capacity and thermal conductivity of the solution, respectively. The heat transfer differential equation of CNC is wtitten as

$$\rho_{CNC} C_{p,CNC} \partial T_{CNC} / \partial t - \nabla \cdot (k_{CNC} \cdot \nabla T_{CNC}) = 0 \tag{S7}$$

The boundary condition is written as

$$-k_{CNC} \partial T / \partial n = -\partial P_Q / \partial S + h \cdot (T_{CNC} - T_s) \tag{S8}$$

where k_{CNC} and h are the thermal conductivity of CNC and the surface heat transfer coefficient, respectively. The item on the left of the equal sign is the effluent heat flux from the surface of CNC, the items on the right of the equal sign are the incident thermal power density and the convective heat flux of surrounding solution, respectively. T_s is the temperature of the solution, which is set as room temperature. P_Q is the thermal power generated by CNC, which is defined as

$$P_Q = \eta \cdot P_{CNC} \tag{S9}$$

where η and P_{CNC} are the total photothermal conversion efficiency of CNC and the total laser power illuminated on CNC, respectively. The thermal source P_Q is set at the phototropic face of CNC. CNC is considered to be homogeneous with same conversion efficiency (η) at each part. Thus, P_Q has the same Gaussian distribution with laser power (P_0).

Figure 3 shows that CNC is quite small compared to the surrounding water domain, so the thermal dynamics process in our case is considered as a convection heat transfer process in large space, the criterion equation is described as

$$Nu = h \cdot L / k_s = C(Gr \cdot Pr)^n \tag{S10}$$

where C and n are empirical constants, L is the typical length. Nu, Gr and Pr are the Nusselt number, Grashof number and Prandtl number, respectively. In our case, the typical length L is set as the outer diameter of CNC. Due to CNC's large aspect ratio, we assume that the thermal convection around the CNC is similar to that around a cylinder. For the micro-sale laminar flow, the empirical constants C and n are determined to be 4.322 and 0.107, respectively.[6] Thus, the surface heat transfer coefficient for laminar flow is written as

$$h = 4.322 k_s \cdot (Gr \cdot Pr)^{0.107} / L \tag{S11}$$

A particle tracing node is added to study the cell motion and position versus time. A fictitious particle that is approximate with the real cell is released near CNC, the effect of cells on the flow field is ignored.

The laser power illuminating on the CNC. As shown in the insert of Figure 2, the laser power is not absorbed by the CNC totally, the power illuminating on the CNC should be calculated. The IR laser beam energy is Gaussian distributed as follows,

$$I(x, y, z) = I_0 \frac{\omega_0^2}{\omega^2(z)} e^{-\frac{2(x^2+y^2)}{\omega^2(z)}} \tag{S12}$$

where I_0 is the intensity of central position, x, y, z are coordinates, $\omega(z)$ is the radius of laser beam

at position z, ω_0 is the radius of focal point at $z=0$. The laser power is expressed as

$$P_0 = \iint_\infty I(x, y, 0)dxdy = \iint_\infty I_0 e^{-\frac{2(x^2+y^2)}{\omega^2(z)}} dxdy = \frac{\pi}{2} I_0 \omega_0^2 \tag{S13}$$

The power illuminating on the CNC is described as

$$P_{CNC} = \iint I_0 e^{-\frac{2(x^2+y^2)}{\omega^2(z)}} dxdy = I_0 \int e^{-\frac{2x^2}{\omega_0^2}} dx \int e^{-\frac{2x^2}{\omega_0^2}} dy \approx \frac{1}{80} P_0 \tag{S14}$$

which shows that there is approximately 1/80 of the IR incident power, as an average of proportion,

can be absorbed by the CNC. The integration range of x and y are the diameter and the length

irradiated by laser of the CNC, respectively.

Using root-mean-square error to determine the optimal values of the simulative values. The

root-mean-square error between the experimental values and simulative values is described as

$$S = [\frac{1}{N} \sum_{i=1}^{N} (x_{i2} - x_{i1})^2]^{\frac{1}{2}}, i = 1, 2, 3, \dots \dots, N \tag{S15}$$

where x_{i2} is the experimental value, x_{i1} is the simulative value, respectively. S is the root-mean-

square error to show the deviation between the experimental values and the simulative values.

Smaller S value means smaller deviation and better match. We contrast the experimental velocities

and simulative velocities corresponding to different P_Q and h values, respectively, at t=10, 20, 30,

40, 50 and 60 ms. The S values corresponding to P_0=76 mW are shown in Table 1.
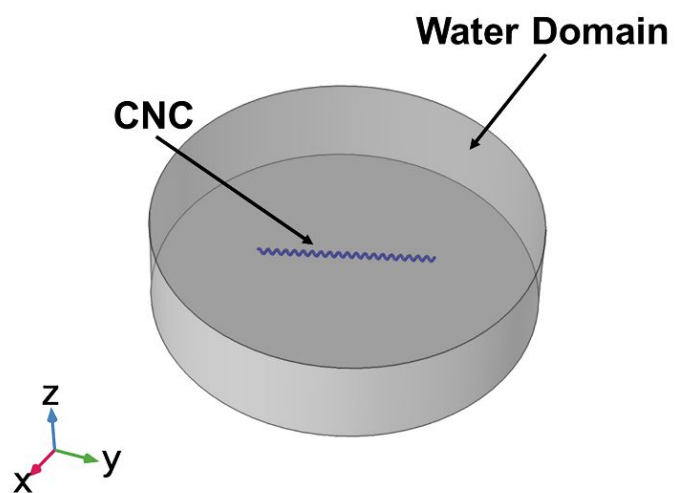
II. Supplementary Figures

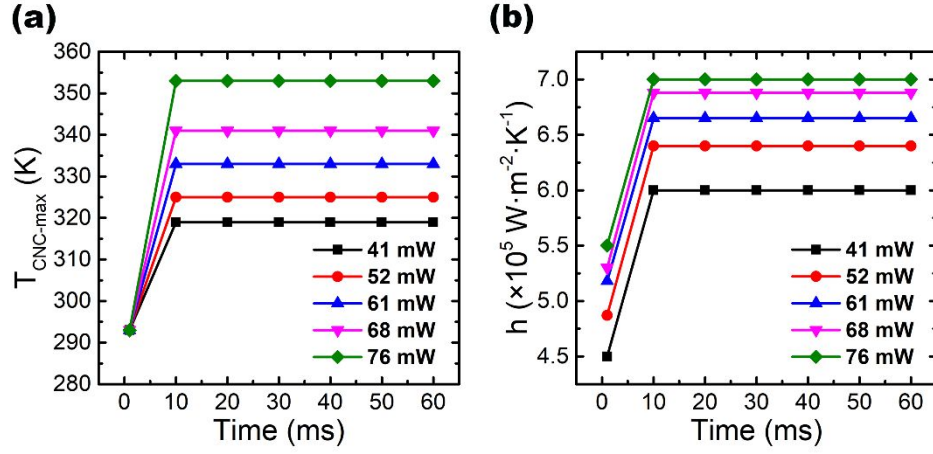**Figure S1.** The 3D stereogram of FEA model.

Figure S2. The variation of the maximum temperature of CNC and the convective heat transfer coefficient versus time. (a) The curves of the maximum temperature of CNC, $T_{CNC-max}$, versus time under different incident laser power P_0. (b) Dependences of the h values on the time under different incident laser power.
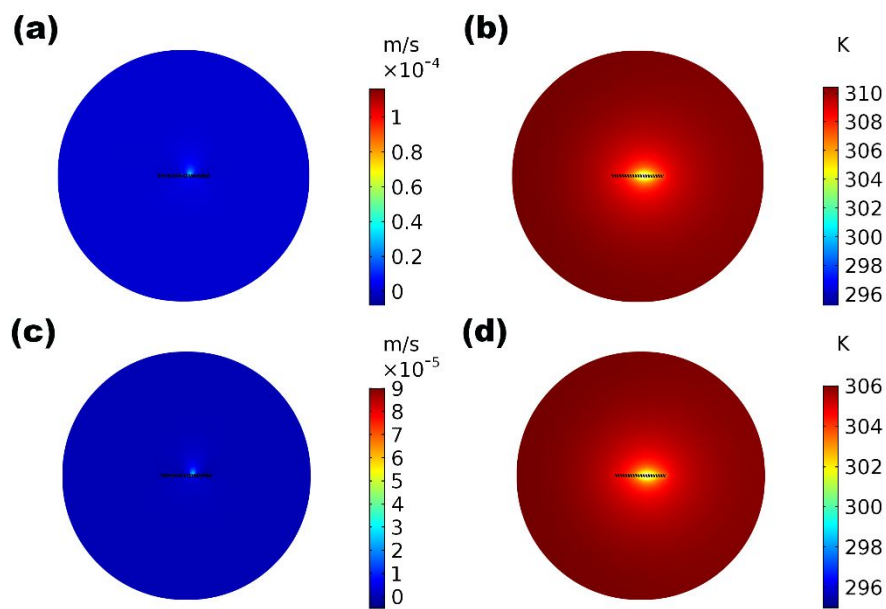
Figure S3. Velocity distribution and temperature distribution of solution domain based on "gold nanocoil", shown in (a) and (b), and "copper nanocoil", shown in (c) and (d), under the P_Q of 0.5 mW. The materials of the nanocoils of set as Au and Cu, respectively. Gold nanocoil and copper nanocoil here have same geometrical parameters with CNC.
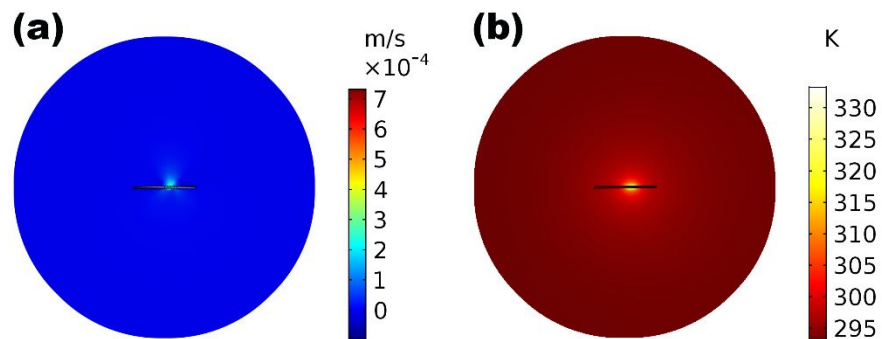
Figure S4. (a) Velocity distribution and (b) temperature distribution of solution domain based on "carbon nanowire" (a straight line with the same physical parameters with CNC) under the P_Q of 0.5 mW.

III. References

1. Howard, H. C.; Hulett, G. A. A Study of the Density of Carbon. *J. Phys. Chem.* **1924**, *28*, 1082-1095.

2. Deng, C. H.; Sun, Y. M.; Pan, L. J.; Wang, T. Y.; Xie, Y. S.; Liu, J.; Zhu, B. W.; Wang, X. W. Thermal Diffusivity of a Single Carbon Nanocoil: Uncovering the Correlation with Temperature and Domain Size. *Acs Nano* **2016**, *10*, 9710-9719.

3. Herwig, H.; Hausner, O. Critical View on "New Results in Micro-Fluid Mechanics": An Example. *Int. J. Heat. Mass. Tran.* **2003**, *46*, 935-937.

4. Gad-el-Hak, M. Comments on "Critical View on New Results in Micro-Fluid Mechanics". *Int. J. Heat. Mass. Tran.* **2003**, *46*, 3941-3945.

5. Eu, B. C. *Kinetic Theory of Nonequilibrium Ensembles, Irreversible Thermodynamics, and Generalized Hydrodynamics*; Springer Cham: Switzerland, 2016.

6. Guan, N.; Liu, Z.; Zhang, C. Natural Convection Heat Transfer for Copper Micro-Wires in Water. *Huagong Xuebao (Chin. Ed.)* **2012**, *63*, 2070-2076.